# Stability and mobility of small vacancy-solute complexes in Fe-MnNi and dilute Fe-X alloys: a kinetic Monte Carlo study.

Messina Luca[a], Lorenzo Malerba[b], Pär Olsson[a]

[a] *KTH Royal Institute of Technology, Reactor Physics, 106 91 Stockholm, Sweden*
[b] *Structural Materials Group, Institute of Nuclear Materials Science, SCK·CEN, Boeretang 200, B-2400 Mol, Belgium*

**Abstract**

Manganese and nickel solute atoms in irradiated ferritic steels play a major role in the nanostructural evolution of reactor pressure vessels (RPV), as they are responsible for the formation of embrittling nanofeatures even in the absence of copper. The stability and mobility of small vacancy-solute clusters is here studied with an atomistic kinetic Monte Carlo approach based on ab initio calculations, in order to investigate the influence of Mn and Ni on the early life of small radiation-induced vacancy clusters, and to provide the necessary parameters for advanced object kinetic Monte Carlo simulations of the RPV long-term nanostructural evolution. Migration barriers are obtained by direct ab initio calculations or through a binding energy model based on ab initio data. Our results show a clear immobilizing and stabilizing effect on vacancy clusters as the solute content is increased, whereas the only evident difference between the two solute species is a somewhat longer elongation of the cluster mean free path in the presence of a few Mn atoms.

*Keywords:* ferritic alloys, AKMC, vacancy diffusion, solute clusters

## 1. Introduction

The influence of manganese and nickel on the microstructural evolution of reactor pressure vessel (RPV) steels under irradiation has recently become of great interest. The observed formation of Mn-Ni-Si-rich nanoclusters is responsible for a possible unexpected acceleration of the RPV embrittlement process and might jeopardize the RPV structural integrity in the long term [1]. The analysis of neutron–irradiated model materials [2, 3, 4] combined with atomistic simulations [5] suggests that such clusters form from the very beginning of irradiation, despite the apparently missing thermodynamic driving force, even in case of low- or no-copper alloys.

The emerging mechanism for the nanocluster formation is segregation of solute atoms (Mn, Ni, Si) on small point-defect (PD) clusters, the mobility of which is progressively reduced by the presence of the solutes themselves. Such complexes act then as sinks for other mobile defects and small defect-solute complexes. As a matter of fact, solute atoms can be transported by defects towards these nucleation sites, causing the clusters to grow in size. The effective "pinning effect" of solute atoms on SIA loops emerges from several studies [6, 7, 8], whereas the systematic arising of a vacancy drag effect in iron dilute alloys has been recently shown [9] to be a very effective means of solute transport towards defect sinks in RPV steels, and could hence confirm this mechanism. In particular, Mn is expected to have a specifically strong effect on SIA–loop mobility because of the strong interaction between Mn and crowdion, in analogy with the effect of Cr [7] and because it is known to efficiently diffuse via a dumbbell mechanism. However, no full nanostructural evolution model has been yet developed to prove that this mechanism actually occurs.

Object kinetic Monte Carlo (OKMC) simulations are a powerful tool to describe the evolution of materials under irradiation up to approximately 1 dpa. In these simulations, the evolution of objects such as single PD, PD clusters and mixed clusters is followed without any atomic–level description of their structure, allowing for better computational efficiency than atomistic kinetic Monte Carlo (AKMC) simulations. The first steps towards the development of an OKMC model for the Fe-MnNi system are described in [10]. The necessary information about the stability and mobility of each object is usually not available experimentally; however, such quantities can be computed via AKMC simulations, as was recently done for Fe–Cu alloys [11, 12, 13].

The objective of this work is therefore to obtain the stability and mobility of small vacancy-solute complexes with AKMC simulations, exclusively based on ab initio–computed binding energies and migration barriers. This study provides a preliminary insight on the effect of Mn and Ni on the small vacancy cluster behavior, as well as the necessary parameters for the development of an OKMC model for dilute Fe-MnNi alloys. In addition, it completes the diffusion study in [9] by providing some kinetic properties of solute–vacancy pairs in iron dilute alloys that could not be obtained with the mean field approach therein applied.

*Email address:* messina@kth.se (Messina Luca)

## 2. Calculation method

### 2.1. AKMC algorithm

The LAKIMOCA code [14] is employed to perform the AKMC simulations. In the AKMC approach, the evolution of the system is modelled as a sequence of vacancy jumps occurring at a rate $\Gamma = \nu \exp(-E_a/k_BT)$, where $\nu$ is the attempt frequency and $E_a$ is the vacancy migration energy. At each jump, the time step is estimated through the residence time algorithm [15].

Clusters containing up to two atoms of each kind and up to four vacancies are here considered. The algorithm used in this work is the same as in [12, 13], where analogous calculations were performed for vacancy-copper clusters. A given cluster is introduced in the center of a 16000-atom simulation box in its assumed most stable configuration (a core of vacancies surrounded by solute atoms progressively filling the nearest neighbor (nn) shells). The position of the cluster center of mass (COM) is tracked until the cluster dissociation. In this work, a cluster is defined by any constituent (other than Fe) being within 5nn distance of each other. In order to gather sufficient statistical data, each simulation (same cluster and temperature) is repeated with $10^2$ to $10^3$ different seeds.

At the end of each stack of calculations, the lifetime is given by the average of the simulation times $\tau^i_{\text{life}}$ at cluster dissociation. The dissociation energy $E_{\text{diss}}$ and the lifetime prefactor $\tau_0$ can be then calculated by linear regression in the Arrhenius domain: $\tau(T) = \tau_0 \exp(E_{\text{diss}}/k_BT)$.

For the diffusion coefficient calculation, the trajectories obtained with different seeds are chained together to form a unique long trajectory. Subsequently, this trajectory is divided in small segments corresponding to a given $\Delta t$. The diffusion coefficient is then computed as:

$$D(T) = \frac{1}{N^{\text{TI}}} \sum_{j=1}^{N^{\text{TI}}} \frac{R_j^2}{6\Delta t_j} \,, \tag{1}$$

where $R_j^2$ is the COM square displacement in segment $j$ and $N^{\text{TI}}$ is the number of segments. Note that the $\Delta t$ of each segment might differ slightly due to the stochastic advancement of the AKMC time. The procedure is repeated for several values of $\Delta t$. The diffusion coefficient $D(T)$ is taken as the average diffusion coefficient in the convergence zone [12]. The migration barrier $E_{\text{mig}}$ and diffusion prefactor $D_0$ are again obtained by linear regression: $D(T) = D_0 \exp(-E_{\text{mig}}/k_BT)$.

Lastly, the mean free path (MFP) of the cluster is obtained from Eq.1:

$$\delta(T) = \sqrt{6D\tau} \,. \tag{2}$$

### 2.2. AKMC parametrization

The activation energies defining the event probability in the AKMC simulations depend on the local atomic environment (LAE) around the exchanging vacancy–atom pair. In this respect, two distinct approaches are here applied for two different sets of simulations.

In the binary dilute limit (only one vacancy and one solute atom in the LAE), a limited amount of jump frequencies is needed; hence the corresponding activation energies can be computed by means of ab initio methods. In [9], a full set of activation energies was obtained for dilute Fe-X alloys with density functional theory (DFT), and the self-consistent mean field method [16] was applied to analyze the drag tendency of a solute atom by a vacancy. However, no information about the migration and the lifetime of the vacancy-solute pair was calculated. Therefore, in the first set of simulations of this work, the Fe-X alloys are simulated in LAKIMOCA by providing the complete table of DFT migration barriers, limited to a 2nn–shell approximation (which entails 10 jump frequencies totally). The mobility and stability of the vacancy-solute pairs are computed, and the results are shown in the following section.

In the general case of a non–dilute alloy, the number of possible LAE configurations is extremely large. In [12, 13], the activation energies were obtained by interpolation with an artificial neural network algorithm on a (large) amount of barriers calculated by means of an interatomic potential. This method is not viable at the moment for the Fe-MnNi system, given the lack of fully reliable interatomic potentials. Therefore, the common final-to-initial-state-energy (FISE) approach is applied:

$$E_{\text{mig}} = E^0_{\text{mig}} + \frac{E_{\text{f}} - E_{\text{i}}}{2} \,. \tag{3}$$

$E^0_{\text{mig}}$ is the reference migration barrier of the jumping species and $E_{\text{i}}$, $E_{\text{f}}$ are the energy of the initial and final configurations. For the latter parameters, pair-interaction cohesive models are usually employed, as done in [17] with DFT-computed properties and fitting on experimental data. Despite the good results obtained in terms of resistivity recovery experiments [18] and cluster precipitation [5], such a model fails in reproducing the drag effect that is dominant at low temperatures [9].

Here the emphasis is on the vacancy–solute interaction, in order to reproduce the drag effect as closely as possible. For this reason, the energy of a given configuration is calculated as the total binding energy between vacancies, Mn and Ni pairs in 1nn and 2nn. The energy difference appearing in Eq.3 is therefore expressed as

$$\Delta E = \sum_{j=1}^{N^{\text{obj}}} \left[ \left( E^{\text{b,i}}_{\text{V}-\text{X}_j} - E^{\text{b,f}}_{\text{V}-\text{X}_j} \right) + \left( E^{\text{b,i}}_{\text{AT}-\text{X}_j} - E^{\text{b,f}}_{\text{AT}-\text{X}_j} \right) \right] \,, \tag{4}$$

where $\text{X}_j$ are all the non-iron objects interacting with the jumping atom (AT) and with the vacancy (V) and $N^{\text{obj}}$ is the amount of such objects.

Jump frequencies also depend on the attempt frequency $\nu$, which is in principle a function of the LAE. Although the migration barrier term is dominant, the attempt frequency might affect solute-vacancy correlations when the differences between migration barriers in the LAE are small, as discussed in [9, 19]. However, the qualitative effect on the cluster stability and mobility tendencies would be negligible. In consideration of the large amount of computational time required for DFT attempt frequency calculations, the Debye frequency ($\nu$ = 6 THz) is assumed throughout this work.

Table 1 provides a complete overview on the DFT data employed in the AKMC parametrization. The binding energies

Table 1: Ab-initio interaction energies between vacancies, Mn and Ni atoms and reference migration energies $E^0_{\mathrm{mig}}$, as calculated in this work or in previous studies [9, 20, 21, 22]. Positive signs stand for attractive (binding) interactions.

| **Interaction energies [eV]** | | | | | | |
|---|---|---|---|---|---|---|
| | V-V [21] | V-Mn [22] | V-Ni [20] | Mn-Mn [22] | Mn-Ni | Ni-Ni [20] |
| 1nn | 0.16 | 0.17 | 0.12 | 0.26 | 0.04 | 0.02 |
| 2nn | 0.23 | 0.11 | 0.20 | -0.02 | -0.01 | 0.01 |
| **Migration energies [eV]** [9] | | | | | | |
| | Fe | Mn | Ni | | | |
| $E^0_{\mathrm{mig}}$ | 0.70 | 0.42 | 0.63 | | | |

were taken from previous DFT calculations [20, 21, 22] , with the exception of the Mn-Ni interaction, which was computed in this work with the Vienna ab initio simulation package VASP [23, 24, 25] and the same parameters as in [20] for the sake of consistency. The reference migration barriers were computed in [9]. The much lower migration barrier for Mn with respect to the previous AKMC parametrization [17] results in time–consuming trapping effects at low temperatures. For this reason, many of the cluster simulations were not performed below 450 K.

## 3. Results and discussion

### *3.1. Vacancy-solute pairs in dilute alloys*

In dilute alloys, vacancy drag affects all solutes observed in radiation–induced nanoclusters (Cu, Mn, Ni, Si, P) at RPV temperatures [9]. This analysis is now extended by calculating the diffusion coefficient, mean lifetime and MFP of the vacancy-solute pairs. The results are shown in Fig.1, while the output of the Arrhenius fitting is reported in Table 2a.

The behavior of Cr is remarkably different due to the lack of interaction with vacancies. Therefore, in dilute Fe(Cr) alloys the vacancy-solute complex is very unstable and does not lead to diffusion of Cr via vacancy drag. In the other cases, the mobility of solute-vacancy pairs is influenced by the combined effect of vacancy-solute exchange rates and kinetic correlations. Specifically, the latter ones reduce the diffusion coefficient of the pair, since the vacancy performs many ineffective jumps (from a diffusion standpoint) as it turns around the solute. For instance, the mobility of the V-Mn complex is larger than that of V-P because of the stronger V-P kinetic correlations, although the solute migration barriers would suggest the opposite trend. In the same way, the V-Cr diffusion coefficient is higher than that of V-Cu and V-Si. Therefore, vacancy drag has the counterintuitive effect of reducing the solute mobility that would be expected in the absence of drag, whereas it has the opposite effect on the solute diffusion coefficient, as was shown in [9].

On the other hand, because of the strong binding tendency, the V-Mn and V-P pairs are remarkably stable. The combination of high stability and fast diffusion leads to very long MFPs, which in the case of P is consistent with the observed heavy segregation at grain boundaries or dislocations [26]. Concerning the other species, the V-Cu and V-Si complexes are more stable than V-Mn and V-Ni because of the larger binding energy (in first approximation $E_{\mathrm{diss}}$ can be estimated as the sum of binding and migration energy [14]),

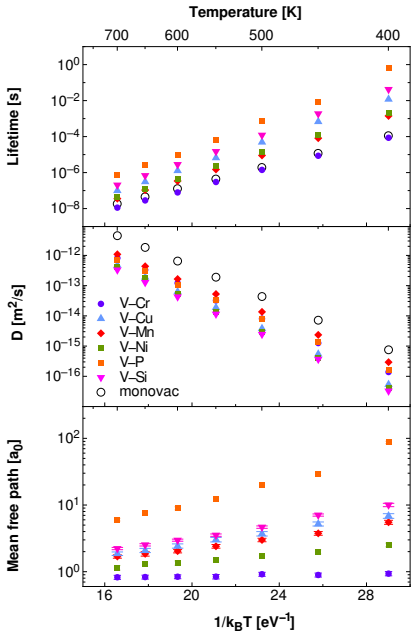


Figure 1: Mean lifetimes, diffusion coefficients and mean free paths of vacancy-solute pairs in dilute binary alloys, as obtained by using the DFT-computed migration barriers in [9] for the AKMC parametrization. The monovacancy lifetime is defined as the average time intercurring between two consecutive vacancy jumps in a pure Fe matrix.

Finally, the computed MFP of the V-Ni pair is shorter than the other solutes with similar drag tendencies (Mn, Cu). This is a direct consequence of the reduced mobility of the V-Ni pair given by the considerably higher migration barrier of Ni with respect to the other solutes. The combination of high stability and short MFP is likely to make Ni especially efficient in reducing the effective diffusion coefficient of the single vacancy, comparable with the more strongly bound Si and Cu.

### *3.2. Vacancy-solute clusters in Fe-MnNi*

The lifetimes, diffusion coefficients and mean free paths as functions of temperature for all analyzed clusters are shown in Fig. 2a, while the results of the linear regression in the Arrhenius domain are listed in Table 2b. The clusters are grouped according to the number of vacancies, to understand how the evolution of a given vacancy cluster is affected by the presence of solutes.

A comparison between the vacancy-solute pairs (V-Mn and V-Ni) of this section and the previous one shows that the binding tendency is well reproduced, as the obtained lifetimes and dissociation energies are comparable. On the other hand, this binding energy model systematically yields smaller diffusion coefficients and MFP's. The reason lies on the sets of Fe-V migration barriers around the solute, which are all larger than the corresponding DFT values. The mobility of such pairs is therefore underestimated.

As far as the $V_xMn_yNi_z$ clusters are concerned, the cluster stability (lifetime and dissociation energy) is enhanced by the addition of solutes in all cases, sometimes significantly. By

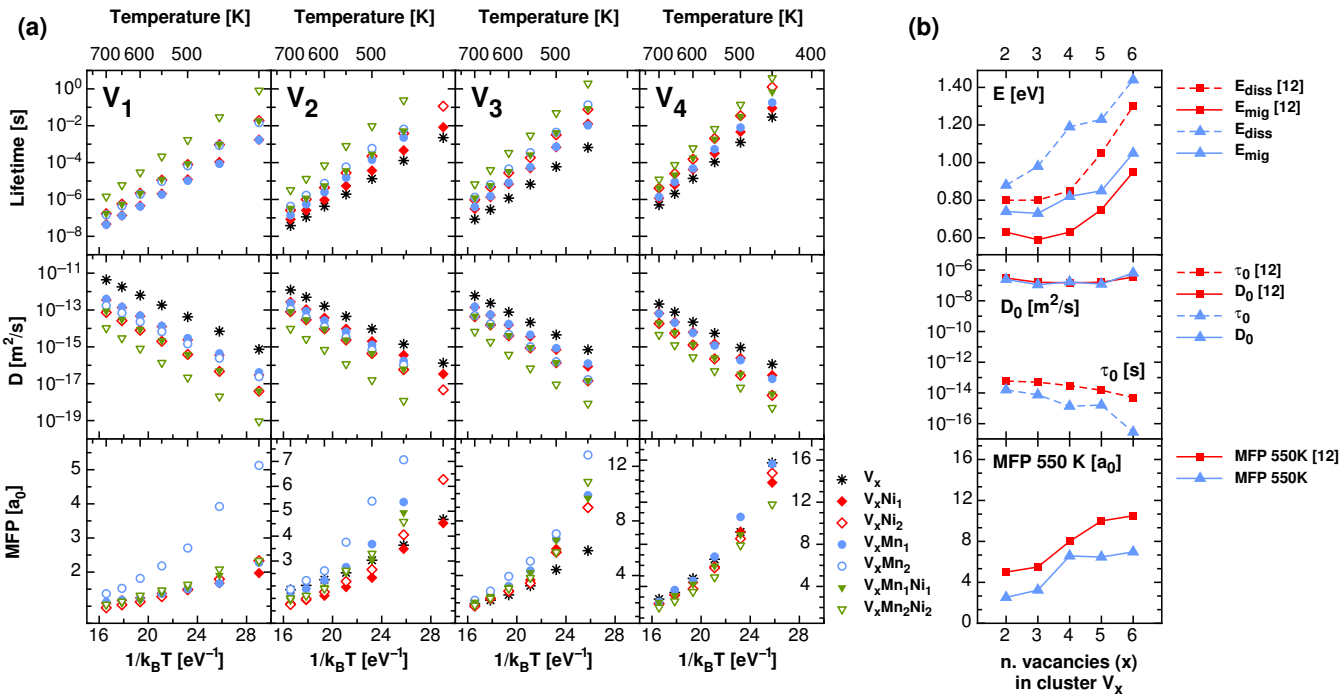


Figure 2: (a) Mean lifetimes, diffusion coefficients and mean free paths of vacancy-solute complexes $V_xMn_yNi_z$ in Fe-MnNi, obtained with AKMC simulations based on the binding energy model for the calculation of migration barriers. (b) Migration and dissociation energies, corresponding prefactors and mean free paths of pure vacancy clusters, obtained in this work (blue lines) and compared to previous calculations (red lines) [13] (colors online).

definition, this model cannot reproduce as much as the previous one the difference in vacancy migration barriers around Ni and Mn solute atoms. For this reason, at this preliminary stage no difference is observed between these two solutes, aside from the isolated case of the $V_2$ clusters, where a single Ni does not seem to affect much the life of the di–vacancy. The addition of undistinguished solute atoms has a strong effect, but no Mn-Ni synergy is found, as the lifetime increment is always given by the superposition of the effect of each species alone.

The expected decrease of diffusion coefficient with increasing cluster size is quite significant (three orders of magnitude when adding four solute atoms). This clearly suggests that small vacancy clusters are severely hindered in their motion when encountering solute atoms. Once more, no visible difference in the behavior of Mn and Ni is observable. The sharp increase of migration energy ensures that the vacancy clusters are slowed down, though not completely immobilized.

The only visible difference between Mn– and Ni-containing clusters is in the MFP: while it is clearly prolonged by Mn, it is not affected (or is even decreased) by Ni atoms. In other words, vacancy clusters show a capability of dragging Mn atoms, which does not apply for Ni. This occurs because the addition of a second Ni solute to the cluster always increases the pair effective migration barrier, while the latter is often lowered by the addition of a second Mn atom. As a consequence, the diffusion coefficient of Ni-containing clusters is smaller and the MFP shorter.

In summary, even at this early stage of the analysis it is possible to establish that the addition of solute atoms systematically increases the stability of the vacancy clusters and decreases their mobility, in some cases at a large extent. On the other hand, it is not possible to observe any significant difference between the influence of Mn and Ni, at such small sizes, in terms of cluster stability and mobility, apart from a clearly longer MFP in presence of Mn. A more systematic approach embracing larger clusters with a smart sampling of the cluster composition (as in [13]), and with a more reliable energy model for the migration barrier calculation, is required in order to analyze more in depth possible disparities between the two solute species. This preliminary study based on few DFT data allows therefore to conclude that Mn and Ni are likely to have a non negligible hampering effect on small vacancy clusters, although the extent of such effect - and the possible total cluster immobilization - cannot be assessed with certainty at this point.

### *3.3. Comparison with previous work*

The results of our calculations are compared to [13] in Fig. 2b, limited to the pure vacancy clusters from two to six elements. The calculations of this study replicate the same trends, which ensures the reliability of the results from a qualitative standpoint. The difference in lifetime (and lifetime prefactor) is due to the more restrictive cut-off condition for cluster dissociation applied in [13] with respect to this work (2nn vs 5nn). On the other hand, the mobility and MFP are here considerably underestimated. It is well known that the di–vacancy and the tri–vacancy are characterized by a lower migration barrier than the monovacancy [27, 21, 13]. In the case of di–vacancies, the dominant migration mechanism was identified in [21]: given

Table 2: Migration energies, dissociation energies, corresponding prefactors and mean free paths at 550 K (in atomic lattice units, $a_0$ = 2.855 Å) for: (a) vacancy-solute pairs in different Fe-X dilute binary alloys, as obtained by using the DFT-computed migration barriers in [9]; (b) vacancy-solute complexes, as obtained by means of the DFT binding-energy model.

| Cluster | $D_0$ ($10^{-8}$ m$^2$/s) | $E_{\mathrm{mig}}$ (eV) | $\tau_0$ ($10^{-15}$ s) | $E_{\mathrm{diss}}$ (eV) | MFP (550 K) ($a_0$) |
|---|---|---|---|---|---|
| **Vacancy-solute pairs in dilute alloys** (a) | | | | | |
| V-Cr | 8.85 ± 0.68 | 0.70 ± 0.003 | 73.2 ± 5.3 | 0.72 ± 0.003 | 0.84 ± 0.06 |
| V-Cu | 9.11 ± 0.69 | 0.73 ± 0.003 | 14.7 ± 2.1 | 0.95 ± 0.007 | 3.03 ± 0.24 |
| V-Mn | 5.89 ± 0.39 | 0.66 ± 0.003 | 29.6 ± 4.4 | 0.84 ± 0.007 | 2.41 ± 0.15 |
| V-Ni | 10.2 ± 1.43 | 0.75 ± 0.006 | 24.4 ± 1.5 | 0.87 ± 0.003 | 1.49 ± 0.10 |
| V-P | 4.95 ± 0.10 | 0.67 ± 0.001 | 7.34 ± 4.86 | 1.10 ± 0.023 | 12.4 ± 0.8 |
| V-Si | 7.03 ± 0.21 | 0.74 ± 0.001 | 17.2 ± 3.5 | 0.98 ± 0.009 | 3.54 ± 0.14 |
| **One-vacancy clusters** (b) | | | | | |
| $V_1$ | 47.3 | 0.70 | | | |
| $V_1Mn_1$ | 7.58 ± 0.32 | 0.74 ± 0.002 | 30.3 ± 6.3 | 0.85 ± 0.008 | 1.37 ± 0.07 |
| $V_1Mn_2$ | 2.34 ± 0.12 | 0.71 ± 0.002 | 27.5 ± 3.2 | 0.93 ± 0.006 | 2.18 ± 0.09 |
| $V_1Ni_1$ | 9.84 ± 0.55 | 0.75 ± 0.002 | 36.2 ± 2.0 | 0.85 ± 0.003 | 1.37 ± 0.05 |
| $V_1Ni_2$ | 3.68 ± 0.23 | 0.79 ± 0.003 | 31.4 ± 1.8 | 0.93 ± 0.003 | 1.28 ± 0.08 |
| $V_1Mn_1Ni_1$ | 5.10 ± 0.43 | 0.80 ± 0.004 | 29.8 ± 3.1 | 0.94 ± 0.005 | 1.39 ± 0.06 |
| $V_1Mn_2Ni_2$ | 5.14 ± 0.68 | 0.93 ± 0.006 | 28.5 ± 4.9 | 1.07 ± 0.008 | 1.46 ± 0.12 |
| **Two-vacancy clusters** (b) | | | | | |
| $V_2$ | 24.8 ± 0.6 | 0.74 ± 0.001 | 16.0 ± 1.1 | 0.88 ± 0.003 | 2.53 ± 0.10 |
| $V_2Mn_1$ | 11.0 ± 0.2 | 0.79 ± 0.001 | 4.13 ± 0.41 | 1.05 ± 0.005 | 2.76 ± 0.11 |
| $V_2Mn_2$ | 2.95 ± 0.45 | 0.76 ± 0.007 | 6.99 ± 2.12 | 1.08 ± 0.014 | 3.76 ± 0.18 |
| $V_2Ni_1$ | 4.46 ± 0.60 | 0.73 ± 0.006 | 16.5 ± 3.2 | 0.93 ± 0.009 | 1.96 ± 0.15 |
| $V_2Ni_2$ | 3.68 ± 0.09 | 0.79 ± 0.001 | 9.50 ± 1.32 | 1.03 ± 0.007 | 2.18 ± 0.10 |
| $V_2Mn_1Ni_1$ | 3.32 ± 0.23 | 0.78 ± 0.003 | 11.2 ± 2.4 | 1.04 ± 0.010 | 2.53 ± 0.12 |
| $V_2Mn_2Ni_2$ | 10.1 ± 1.0 | 0.98 ± 0.005 | 4.59 ± 2.05 | 1.22 ± 0.019 | 2.61 ± 0.20 |
| **Three-vacancy clusters** (b) | | | | | |
| $V_3$ | 11.2 ± 0.4 | 0.73 ± 0.002 | 7.51 ± 1.22 | 0.98 ± 0.008 | 3.24 ± 0.14 |
| $V_3Mn_1$ | 5.38 ± 0.46 | 0.77 ± 0.004 | 3.44 ± 0.72 | 1.12 ± 0.010 | 4.35 ± 0.26 |
| $V_3Mn_2$ | 10.2 ± 1.0 | 0.87 ± 0.004 | 1.41 ± 0.32 | 1.25 ± 0.010 | 5.05 ± 0.32 |
| $V_3Ni_1$ | 8.89 ± 0.60 | 0.80 ± 0.003 | 1.69 ± 0.27 | 1.15 ± 0.008 | 2.95 ± 0.19 |
| $V_3Ni_2$ | 8.83 ± 0.71 | 0.87 ± 0.004 | 1.58 ± 0.52 | 1.22 ± 0.014 | 3.44 ± 0.20 |
| $V_3Mn_1Ni_1$ | 8.68 ± 0.56 | 0.87 ± 0.003 | 2.19 ± 0.45 | 1.21 ± 0.009 | 4.20 ± 0.22 |
| $V_3Mn_2Ni_2$ | 6.91 ± 1.92 | 0.98 ± 0.012 | 1.46 ± 0.54 | 1.34 ± 0.016 | 3.83 ± 0.29 |
| **Four-vacancy clusters** (b) | | | | | |
| $V_4$ | 17.1 ± 1.2 | 0.82 ± 0.003 | 1.37 ± 0.21 | 1.19 ± 0.007 | 6.58 ± 0.36 |
| $V_4Mn_1$ | 15.1 ± 1.3 | 0.88 ± 0.004 | 0.94 ± 0.42 | 1.28 ± 0.018 | 6.83 ± 0.44 |
| $V_4Ni_1$ | 7.03 ± 0.35 | 0.84 ± 0.002 | 1.77 ± 0.50 | 1.23 ± 0.012 | 5.89 ± 0.39 |
| $V_4Ni_2$ | 20.0 ± 1.0 | 0.98 ± 0.002 | 0.54 ± 0.15 | 1.37 ± 0.012 | 5.76 ± 0.33 |
| $V_4Mn_1Ni_1$ | 18.4 ± 1.5 | 0.97 ± 0.004 | 1.18 ± 0.47 | 1.33 ± 0.017 | 5.94 ± 0.37 |
| $V_4Mn_2Ni_2$ | 5.72 ± 0.43 | 0.99 ± 0.003 | 1.28 ± 0.30 | 1.39 ± 0.011 | 4.87 ± 0.31 |
| **Larger pure vacancy clusters** (b) | | | | | |
| $V_5$ | 12.1 ± 1.7 | 0.85 ± 0.006 | 1.63 ± 0.33 | 1.23 ± 0.008 | 6.47 ± 0.42 |
| $V_6$ | 64.4 ± 9.6 | 1.05 ± 0.006 | 0.28 ± 0.07 | 1.44 ± 0.010 | 6.97 ± 0.39 |

the higher stability of the 2nn configuration and a particular combination of jump frequencies, the di-vacancy can easily switch from 2nn to 4nn and diffuse through the lattice. Evidently, this mechanism is not well reproduced by our binding energy model. A close look to the migration barriers for a di-vacancy complex reveals that the $\omega_{2nn\rightarrow 4nn}$ frequency is excessively large compared to the DFT value [21] and this atypical diffusion mechanism is therefore impeded. Moreover, the more common 1nn-2nn mechanism described in [27] is also underestimated, as the migration barriers predicted by our model are not significantly lower than the background barrier, as is the case for the DFT values [21]. A more accurate energy model is therefore needed in order to reproduce the correct behavior of vacancy clusters in bcc Fe and confirm the extent of the vacancy cluster immobilization and stabilization. At any rate, this does not affect the conclusions about the effect of solutes on vacancy cluster mobility, as the effect is relative to the case of pure vacancy clusters with no solutes.

## 4. Conclusions

The stability and mobility of vacancy-solute pairs in dilute alloys and of small vacancy-solute complexes was quantitatively analyzed with AKMC simulations. For the dilute alloys, DFT-calculated migration barriers were directly introduced in the AKMC code, whereas for the Fe-MnNi alloy the migration barriers were obtained with a DFT binding energy model including interactions between vacancies, Mn and Ni.

In the dilute case, the results complete the vacancy-solute interaction analysis performed in [9] and show that, even if the drag tendency is equally strong, the dissociation energy and mean free path of the various solute-vacancy pairs are considerably different. As for the Fe-Mn-Ni alloy, the trends in terms of mobility and stability of vacancy clusters of increasing size are in good agreement with previous calculations. This work shows that even the presence of few solute atoms in the vacancy clusters reduces their mobility and increases their stability significantly. Such considerable effect raises the interest for the development of a more accurate AKMC model, which will be the object of future work, in order to estimate the change of vacancy cluster mobility and stability as function of Mn and Ni concentration. The final output will provide the necessary parameters for the development of OKMC models, which in turn will give valuable insights on the formation, growth and long-term evolution of the embrittling nanofeatures in RPV steels.

## Acknowledgments

This work was accomplished thanks to the financial support from Vattenfall, the Göran Gustafsson Foundation and the European Commission, in the framework of the MatISSE project under Grant No. 604862. It contributes to the Joint Programme on Nuclear Materials (JPNM) of the European Energy Research Alliance (EERA). The authors acknowledge N. Castin, M. I. Pascuet, C. Domain and M. Nastar for their valuable contributions.

[1] G. R. Odette, R. K. Nanstad, Predictive Reactor Pressure Vessel Steel Irradiation Embrittlement Models: Issues and Opportunities, JOM 61 (7) (2009) 17–23.

[2] E. Meslin, M. Lambrecht, M. Hernández-Mayoral, F. Bergner, L. Malerba, P. Pareige, B. Radiguet, A. Barbu, D. Gómez-Briceño, A. Ulbricht, A. Almazouzi, Characterization of neutron-irradiated ferritic model alloys and a RPV steel from combined APT, SANS, TEM and PAS analyses, J. Nucl. Mat. 406 (1) (2010) 73–83.

[3] E. Meslin, B. Radiguet, P. Pareige, C. Toffolon, A. Barbu, Irradiation-Induced Solute Clustering in a Low Nickel FeMnNi Ferritic Alloy, Exp. Mech. 51 (9) (2011) 1453–1458.

[4] E. Meslin, B. Radiguet, M. Loyer-Prost, Radiation-induced precipitation in a ferritic model alloy: An experimental and theoretical study, Acta Mater. 61 (16) (2013) 6246–6254.

[5] R. Ngayam-Happy, C. S. Becquart, C. Domain, L. Malerba, Formation and evolution of MnNi clusters in neutron irradiated dilute Fe alloys modelled by a first principle-based AKMC method, J. Nucl. Mat. 426 (1-3) (2012) 198–207.

[6] J. Marian, B. Wirth, J. Perlado, Mechanism of Formation and Growth of 100 Interstitial Loops in Ferritic Materials, Phys. Rev. Lett. 88 (25) (2002) 255507.

[7] D. Terentyev, L. Malerba, A. V. Barashev, On the correlation between self-interstitial cluster diffusivity and irradiation-induced swelling in Fe–Cr alloys, Philos. Mag. Lett. 85 (11) (2005) 587–594.

[8] N. Anento, A. Serra, submitted to Nucl. Instrum. Methods Phys. Res. B (2014).

[9] L. Messina, P. Olsson, M. Nastar, T. Garnier, C. Domain, Exact ab initio transport coefficients in bcc Fe-X (X=Cr, Cu, Mn, Ni, P, Si) dilute alloys, Phys. Rev. B 90 (2014) 104203.

[10] M. Chiapetto, C. S. Becquart, C. Domain, L. Malerba, Nanostructure evolution under irradiation of Fe(C)MnNi model alloys for reactor pressure vessel steels, submitted to Nucl. Instrum. Methods Phys. Res. B (2014).

[11] F. G. Djurabekova, L. Malerba, C. Domain, C. S. Becquart, Stability and mobility of small vacancy and copper-vacancy clusters in bcc-Fe: An atomistic kinetic Monte Carlo study, Nucl. Instrum. Methods Phys. Res. B 255 (1) (2007) 47–51.
[12] M. I. Pascuet, N. Castin, C. S. Becquart, L. Malerba, Stability and mobility of Cu–vacancy clusters in Fe–Cu alloys: A computational study based on the use of artificial neural networks for energy barrier calculations, J. Nucl. Mat. 412 (1) (2011) 106–115.
[13] N. Castin, M. I. Pascuet, L. Malerba, Mobility and stability of large vacancy and vacancy-copper clusters in iron - An atomistic kinetic Monte Carlo study, J. Nucl. Mat. 429 (1-3) (2012) 315–324.
[14] C. Domain, C. S. Becquart, L. Malerba, Simulation of radiation damage in Fe alloys: an object kinetic Monte Carlo approach, J. Nucl. Mat. 335 (1) (2004) 121–145.
[15] A. B. Bortz, M. H. Kalos, J. L. Lebowitz, A new algorithm for Monte Carlo simulation of Ising spin systems, J. Comp. Phys. 17 (1) (1975) 10–18.
[16] M. Nastar, A mean field theory for diffusion in a dilute multi-component alloy: a new model for the effect of solutes on self-diffusion, Phil. Mag. 85 (32) (2005) 3767–3794.
[17] E. Vincent, C. S. Becquart, C. Domain, Microstructural evolution under high flux irradiation of dilute Fe-CuNiMnSi alloys studied by an atomic kinetic Monte Carlo model accounting for both vacancies and self interstitials, J. Nucl. Mat. 382 (2-3) (2008) 154–159.
[18] R. Ngayam-Happy, P. Olsson, C. S. Becquart, C. Domain, Isochronal annealing of electron-irradiated dilute Fe alloys modelled by an ab initio based AKMC method: Influence of solute-interstitial cluster properties, J. Nucl. Mat. 407 (1) (2010) 16–28.
[19] T. Garnier, M. Nastar, P. Bellon, D. R. Trinkle, Solute drag by vacancies in body-centered cubic alloys, Phys. Rev. B 88 (2013) 134201.
[20] P. Olsson, T. P. C. Klaver, C. Domain, Ab initio study of solute transition-metal interactions with point defects in bcc Fe, Phys. Rev. B 81 (5) (2010) 054102.
[21] F. Djurabekova, L. Malerba, R. C. Pasianot, P. Olsson, K. Nordlund, Kinetics versus thermodynamics in materials modeling: The case of the di-vacancy in iron, Phil. Mag. 90 (19) (2010) 2585–2595.
[22] A. Bakaev, D. Terentyev, G. Bonny, T. P. C. Klaver, P. Olsson, D. Van Neck, Interaction of minor alloying elements of high-Cr ferritic steels with lattice defects: An ab initio study, J. Nucl. Mat. 444 (1-3) (2014) 237–246.
[23] G. Kresse, J. Hafner, Ab initio Molecular-Dynamics for Liquid-Metals, Phys. Rev. B 47 (1) (1993) 558–561.
[24] G. Kresse, J. Hafner, Norm-Conserving and Ultrasoft Pseudopotentials for First-Row and Transition-Elements, J. Phys.: Condens. Matter 6 (40) (1994) 8245–8257.
[25] G. Kresse, J. Hafner, Ab-Initio Molecular-Dynamics Simulation of the Liquid-Metal Amorphous-Semiconductor Transition in Germanium, Phys. Rev. B 49 (20) (1994) 14251–14269.
[26] M. K. Miller, K. A. Powers, R. K. Nanstad, P. Efsing, Atom probe tomography characterizations of high nickel, low copper surveillance RPV welds irradiated to high fluences, J. Nucl. Mat. 437 (1-3) (2013) 107–115.
[27] C. C. Fu, J. Dalla Torre, F. Willaime, J. L. Bocquet, A. Barbu, Multiscale modelling of defect kinetics in irradiated iron, Nat. Mater. 4 (1) (2005) 68–74.